Available online at www.sciencedirect.com
SCIENCE DIRECT®
Applied Catalysis B: Environmental 49 (2004) 207–215
APPLIED CATALYSIS B: ENVIRONMENTAL
www.elsevier.com/locate/apcatb

Bleaching and photobleaching of Orange II within seconds by the oxone/Co^{2+} reagent in Fenton-like processes

Javier Fernandez [a], Pichai Maruthamuthu [b], Albert Renken [c], John Kiwi [a,*]

[a] *Laboratory of Photonics and Interfaces, ICMB-SB, Swiss Federal Institute of Technology (EPFL), Lausanne 1015, Switzerland*
[b] *Department of Energy, University of Madras, Chennai 600025, India*
[c] *Laboratory of Chemical Reaction Engineering, ICMB-SB, Swiss Federal Institute of Technology, Lausanne 1015, Switzerland*

Received 6 July 2003; received in revised form 10 November 2003; accepted 11 December 2003

Abstract

Accelerated bleaching, photobleaching and mineralization of the non-biodegradable azo-dye, Orange II, was observed with oxone in solutions with Co^{2+}-ions. The bleaching rate of Orange II in the dark was found to follow a first-order kinetics with respect to [Co^{2+}] with a rate constant of 20 M^{-1} s^{-1}. Fitting of the Orange II photobleaching experimental points in the presence of the Co^{2+}/oxone reagent was carried out and followed the trend known for reactions presenting a chain radical branched mechanism. The photobleaching trace could be fitted by a single mathematical expression with an error <5% with respect to the experimental data. The bleaching trace observed for the Orange II solution in the dark followed zero-order decay kinetics. In a typical run, Orange II (0.20 mM or TOC 30 mg C/l) in the presence of oxone and Co^{2+} was bleached under visible light within ∼15 s. The Co^{2+}-ion concentrations necessary to catalyze the Orange II mineralization by oxone was observed to be ∼100 times lower than the oxone concentration. A 100% TOC decrease, under visible light irradiation, was attained for an Orange II (0.2 mM) solution in the presence of Co^{2+}-ions (0.06 mM) and oxone (20 mM) within times ∼70 min for solutions purged with oxygen. Under visible light irradiation, Orange II mineralization in the presence of O_2 involves the photo-dissociation of reaction intermediates leading to organic peroxides in the second step of the mineralization process.

Keywords: Bleaching; Photobleaching; Mineralization; Orange II; Oxone; Sulfate radicals; Visible light; Co^{2+}-ions; Stopped-flow; Modeling; Branched radical chains; O_2-effect

1. Introduction

The degradation of dyes has become increasingly important during the last decade in the field of Advanced Oxidation Technologies (AOT's) [1–5]. Azo-dyes like Orange II represent more than 15% of the world production of dyes used in the textile manufacturing industry. These dyes are for the most part non-biodegradable and toxic and at present are abated by some common non-destructive processes [1,2]. The bleaching and mineralization of dyes in short treatment times have not been achieved for most of them investigated so far, posing a serious drawback from the economic point of view with regard to the practical application of AOT's. Only short treatment times when using expensive photons and oxidant(s) in a suitable reactor will allow AOT's treatments to compete with the more traditional non-destructive technology. Several techniques such as Fenton [6], photo-Fenton [7] and TiO_2 photocatalysis [8] have been used to abate the model azo-dye, Orange II.

The mineralization of pollutants has been carried out in recent years using peroxodisulfates as oxidants in the presence of TiO_2 in the AOT's field [6,8–10]. Malato et al. [11] have successfully tested peroxodisulfate ($S_2O_8^{2-}$) and oxone ($2KHSO_5{\cdot}KHSO_4{\cdot}K_2SO_4$) which is essentially HSO_5^- and also known as peroxomonosulfate (PMS). This oxidant has been used in the degradation of pentachlorophenol under visible light irradiation in conjunction with a TiO_2 oxidant as an alternative to H_2O_2 which is widely used for this purpose. Oxone has been successfully used in dark and photochemical reactions [12] like: olefin epoxydations [13,14], chemiluminescence detection of oxidative processes [15] and diverse sulfate oxidation reactions [16]. Catalytic decomposition of oxone (PMS) in the presence of some semiconductors WO_3, Bi_2O_3 and Fe_2O_3 [17,18] and metallic-ions like Mn^{2+}

* Corresponding author. Tel.: +41-21-693-3621; fax: +41-21-693-3621.
E-mail address: john.kiwi@epfl.ch (J. Kiwi).

0926-3373/$ – see front matter © 2004 Elsevier B.V. All rights reserved.
doi:10.1016/j.apcatb.2003.12.018

[19], Cu^{2+} [20] and Co^{2+} [21,22] has also been recently reported.

The Fenton reagent is used as a common source of $HO^{\bullet}$ and $HO_2^{\bullet}$ radicals besides other oxidative intermediates in aqueous solutions. AOT's [10–12] uses UV-Vis light to activate the degradation of many organic compounds through the formation of metallo-complexes like: ligand to metal (LMCT), metal to ligand or ligand to ligand (LLCT) charge transfer photo-dissociation states leading to a variety of radicals under light irradiation [6–10,21,23,24]. Ozone has also been used as a source of oxidative radicals in waste water treatment [2]. Oxone (HSO_5^-) which is a mono-SO_3^- substituted HOOH, has not been widely used as an oxidant during the abatement of pollutants. Reaction (2) proceeds at a very high potential, but the reaction is very slow. No direct measure for the oxidation potential is known for reaction (4). The values given below for reaction (4) are calculated potentials from equilibria considerations. Details of reactions ((2)–(4)) have been reported [11,17,21]:

$$H_2O_2 \rightarrow 2HO^{\bullet}, \quad E^0 = 1.76\,\text{eV} \tag{1}$$

$$S_2O_8^{2-} \rightarrow 2SO_4^{\bullet 2-}, \quad E^0 = 2.12\,\text{eV} \tag{2}$$

$$S_2O_8^{2-} + e^- \rightarrow SO_4^{\bullet 2-} + SO_4^{\bullet -}, \quad E^0 = 2.00\,\text{eV} \tag{3}$$

$$SO_4^{\bullet -} + e^- \rightarrow SO_4^{2-}, \quad E^0 = 2.5\text{–}3.1\,\text{eV} \tag{4}$$

The present investigation addresses the bleaching and mineralization of Orange II in the presence of a Co^{2+}/oxone reagent. Oxone should be a suitable oxidant because it has a higher potential than H_2O_2 ($E^0 = 1.82$ V versus $E^0 = 1.76$ V) [12–14]. In the presence of metal-ions, oxone is known to generate $SO_5^{\bullet -}$ and $SO_4^{\bullet -}$ in aqueous solution in addition to $HO^{\bullet}$ radicals through radical chain reactions [17,21]. The oxidation potential 1.82 eV of oxone is slightly higher than the oxidation potential of 1.80 eV of the couple Co^{3+}/Co^{2+} suggesting that a low overpotential is able to drive the reaction to Co^{3+} from the initial Co^{2+}-ion upon oxone addition in solution. The oxidation of Co^{2+} by oxone to the unstable Co^{3+} due to its high reactivity in an aqueous solution has been reported [18,19,25,26]. Solutions of Co^{3+}-ions have also been prepared by electrochemical oxidation of Co^{2+} [19,20].

2. Experimental section

2.1. Materials

Orange II solutions were prepared by dissolving the sodium salt of this dye (Fluka) and Co^{2+} solutions were prepared from $CoSO_4 \cdot 7H_2O$ p.a. Fluka AG. The Oxone® solutions were prepared from [$2KHSO_5 \cdot KHSO_4 \cdot K_2SO_4$], Aldrich Catalogue No. 22803-6. Reactions were performed by mixing appropriate concentrations of Orange II, Co-salt and oxone in this order, immediately before irradiation.

2.2. Irradiation reactor and procedures

Solar simulated light was applied on cylindrical Pyrex reactor vessels (60 ml), each time using appropriate solutions of the dye, metal-ion and oxone. Light irradiation was carried out by means of a Hanau Suntest lamp (AM1, tunable in light intensity) equipped with an IR filter to remove the infrared radiation. The radiant flux of the Suntest solar simulator was measured with a power-meter from the YSI Corp., Colorado, USA. The short wavelength radiation ($\lambda < 310$ nm) was removed by the Pyrex wall of the reaction vessels. The Orange II discoloration reactions were followed by measuring the optical density (OD) at the maximum of Orange II absorption ($\lambda = 486$ nm) in a Hewlett-Packard 38620 N diode array spectrophotometer. The total organic carbon (TOC) of the solutions was measured by a Shimadzu 500 TOC analyzer. The sulfate concentration was followed using a Dionex DX-100 Ion Chromatograph, provided with an IonPac AS14 column. The eluent consisted of a solution containing sodium carbonate (3.5 mM) and Na-bicarbonate (1 mM).

2.3. Stopped-flow experiments

Fig. 1 shows the set-up used to carry out the experiments reported in Figs. 4–6. The light source was a polychromatic Osram 450 W Xe-lamp with 160 mW/cm^2 and it was used as both the excitation and reference light beam at different regions of the spectra in each case.

In the stopped-flow instrument from Applied Photophysics (Model No. SFA-11), the sample was injected into a 2 mm sample cell. In this way, it was possible to trigger the oscilloscope at the same time as the mixing of the Orange II solution with the oxone (since they do not react in the second time scale) and monitor the reaction from time zero when the Co^{2+}-ion solution is added to the mixture. The band-pass filter (1) and interference filter were selected to isolate the band(s) of interest in the spectral region that allows the quantification of the difference between the excitation and the detection beam. If a narrow band-pass filter was used practically no light entered the system. If a wide band-pass filter was used the IR and the UV-c and UV-b

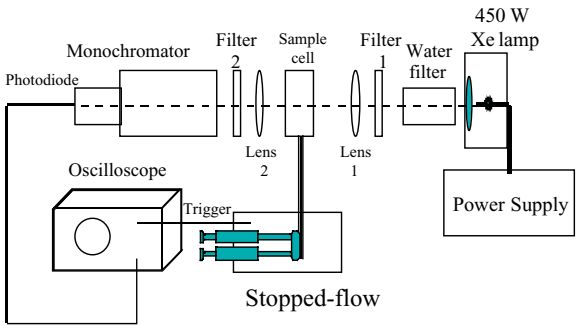

Fig. 1. Schematic representation of the stopped-flow systems used to follow the photobleaching of Orange II in the presence of oxone and Co^{2+}. For other details see text.

regions were blocked, but variations of the light level at $\lambda = 486$ nm could be detected. The detection wavelength at $\lambda = 486$ nm was chosen for analysis and kept constant when following the photobleaching. The lens was used to focus (1) the light from the 450 W Osram Xe-lamp onto the sample and (2) the light on the entrance slit of the monochromator. Filter (2) was the second band-pass filter to isolate the appropriate spectral regions reaching the Baush and Lomb monochromator UV-blazed at 350 nm. The monochromator light was measured by a silicon photodiode (Oriel 71883, 100 kHz, DC 9). Finally, a Tektronix TDS 640 double beam oscilloscope was used for data recording and storage. The first channel was used to detect the signals that were converted in a second step as variations in optical densities. The second channel was used to trigger the system. The absorption changes (A) registered in the oscilloscope were fed into a power Macintosh.

3. Results and discussion

3.1. Orange II bleaching monitored by stopped-flow effect of cobalt and Orange II concentrations

Accelerated bleaching was observed for Orange II (noted as R-H in the scheme below) when the concentration of Co^{2+} was increased from 0.03 to 1.54 mM in the presence of oxone (20 mM). Considering the main reactions involving the sulfate radicals from the peroxone in solution [21]:

$$Co^{2+} + H_2O \Leftrightarrow CoOH^+ + H^+, \quad K_5 \tag{5}$$

$$CoOH^+ + HSO_5^- \rightarrow CoO^+ + H_2O + SO_4^{\bullet -}, \quad k_6 \tag{6}$$

$$CoO^+ + 2H^+ \Leftrightarrow Co^{3+} + H_2O, \quad K_7 \tag{7}$$

$$SO_4^{\bullet -} + Co^{2+} \rightarrow SO_4^{2-} + Co^{3+}, \quad k_8 \tag{8}$$

$$R\text{-}H + SO_4^{\bullet -} \rightarrow R\text{-}H^+ + SO_4^{2-}, \quad k_9 \tag{9}$$

From (5) it is possible to state that

$$[CoOH^+] = \frac{K_5[Co^{2+}]}{[H^+]} \tag{10}$$

and from Eq. (9) it follows:

$$\frac{-d[R\text{-}H]}{dt} = k_9[R\text{-}H][SO_4^{\bullet -}],$$

$$\frac{d[SO_4^{2-}]}{dt} = \frac{k_6K_5[Co^{2+}][HSO_5^-]}{[H^+]} - k_8[Co^{2+}][SO_4^{\bullet -}] - k_9[R\text{-}H][SO_4^{\bullet -}] = 0 \tag{11}$$

and in the steady state $[SO_4^{\bullet -}] = k_6K_5[Co^{2+}][HSO_5^-]/([H^+](k_8[Co^{2+}] + k_9[R\text{-}H]))$ and inserting this expression in (11):

$$\frac{-d[R\text{-}H]}{dt} = \frac{k_9k_6K_5[Co^{2+}][HSO_5^-][R\text{-}H]}{[H^+](k_8[Co^{2+}]k_9[R\text{-}H])} \tag{12}$$

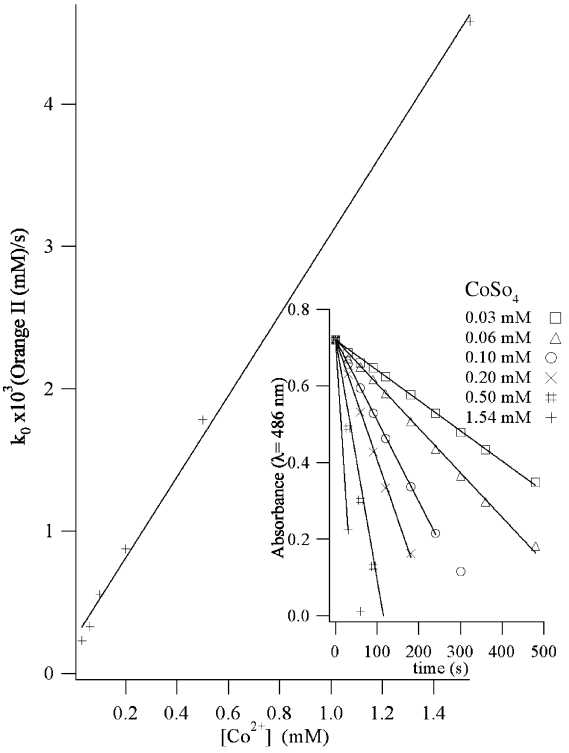

Fig. 2. Plot of the zero-order reaction constant between Orange II (0.20 mM) and oxone (20 mM) in the dark as a function of Co^{2+}-ion concentration added in solution at pH 2. The inset shows the bleaching of Orange II solutions for different Co^{2+} concentrations.

Fig. 2 (inset) shows that a zero-order bleaching is obtained with respect to Orange II (R-H), and that for various $CoSO_4$ concentrations (oxidant in the net sense) it decreases within seconds. The observed decrease is in direct relation to the concentration of $CoSO_4$ used. The zero-order kinetics can be understood taking into account $k_9[R\text{-}H] \gg k_8[Co^{2+}]$ at a defined concentration of HSO_5^-. The limiting rate in the sequence of reactions (5)–(9) is the production of sulfate radicals in reaction (6). Since reaction (9) is kinetically faster than reaction (8), the bleaching of Orange II (Fig. 2) follows:

$$\frac{-d[R\text{-}H]}{dt} = k_{Co}[Co^{2+}] \tag{13}$$

where $k_{Co} = k_9k_6K_5[HSO_5^-][R\text{-}H]/[H^+](k_8[Co^{2+}] + k_9[R\text{-}H])$. The numerical value for k_{Co} in Eq. (13) is 2.8×10^{-3} molecules Orange II/(atom Co^{2+} s). At a defined Co^{2+} concentration, the zero-order bleaching reaction in Fig. 2 can be written as

$$\frac{-d[R - H]}{dt} = k_0 \tag{14}$$

Considering the $[Co^{2+}]$ constant in Eq. (12) when the concentration of Orange II is increased, the numerator in this equation increases more than the denominator. Therefore, k_0 will slightly increase with a higher Orange II concentration, this is shown in Fig. 3. Figs. 2 and 3 show that bleaching

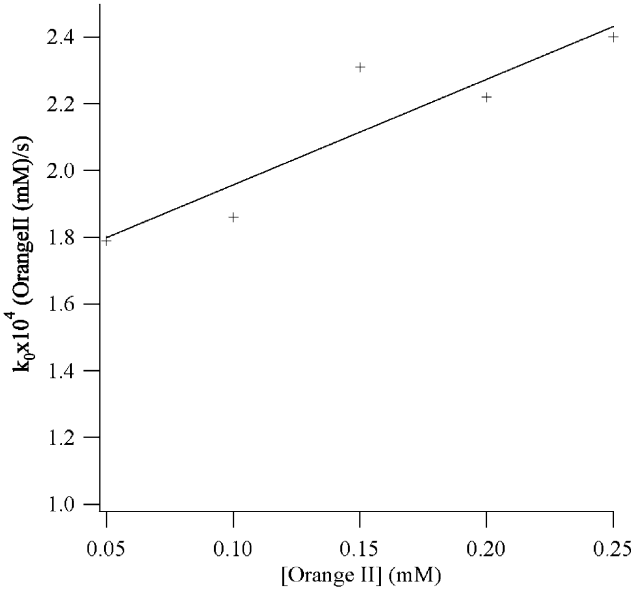

Fig. 3. Reciprocal plot of the zero-order rate for Orange II bleaching as a function of Orange II concentration in the presence of Co^{2+} (0.04 mM) and oxone (5.40 mM).

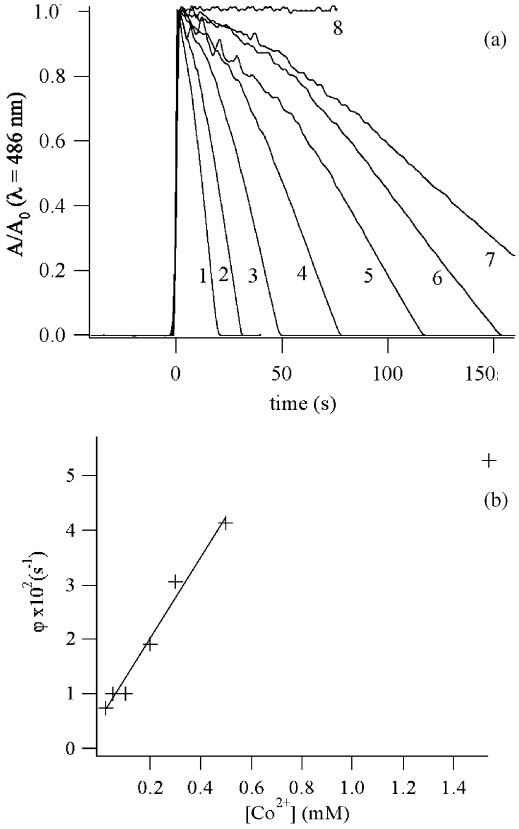

Fig. 4. (a) Photobleaching of an Orange II (0.2 mM) solution in the presence of oxone (40 mM) and various Co^{2+} concentrations: (1) 1.54 mM, (2) 0.5 mM, (3) 0.3 mM, (4) 0.2 mM, (5) 0.1 mM, (6) 0.05 mM, (7) 0.025 mM and (8) no Co^{2+}. (b) Branching parameter plotted against the Co^{2+} concentration during the photobleaching of Orange II (0.20 mM). For other details see text.

in the dark involves the coupling of oxone and Co^{2+}. The cobalt-ions in solution catalyze the decomposition of oxone (reaction (6)) and the limiting step is not the reaction of Orange II with the radicals in solution, but is set by the generation of the radicals themselves in the solution.

The radical–radical termination reactions and the role of $-SO_5^-$ have not been included in Eqs. (5)–(14) since we wanted to arrive at a simplified scheme that could be related to the experimental results presented in this study.

3.2. Effect of the cobalt and oxone concentrations on the photobleaching of Orange II monitored by stopped-flow

Photobleaching of Orange II were investigated in the set-up shown in Fig. 1 by the disappearance of Orange II following the peak absorption at $\lambda = 486$ nm. Control experiments show that no bleaching, photobleaching or mineralization of Orange II in the presence of Co^{2+} or oxone occurs when both reagents were added separately to an Orange II solution in the stopped-flow set-up. Also, the photolysis of Orange II in the presence of Co^{2+} or oxone alone, did not lead to Orange II photobleaching. No change in the spectrum of Orange II was observed upon addition of Co^{2+}, ruling out the possibility of any complex formation between Co^{2+} and Orange II the absence of oxone.Fig. 4a shows the photobleaching of Orange II under Xe-light monitored in the set-up (Fig. 1) by adding different concentrations of Co^{2+}-ions. The Orange II photobleaching traces present a trend similar to the trend observed in processes involving a radical chain branching mechanism [22,23]. Fig. 4a shows that no photobleaching takes place when Co^{2+}-ions are absent suggesting that the chain radical branched reaction only occurs when the oxone decomposition is mediated by Co^{2+}-ions. When the oxone and Co^{2+} are added in solutions containing organic compound(s), the formation of peroxides (ROOH) in radical chain processes have been reported [6,8,9]:

$$R^\bullet + O_2 \rightarrow RO_2^\bullet \quad (15)$$

$$RO_2^\bullet + R\text{-}H \rightarrow ROOH + R^\bullet \quad (16)$$

and the peroxide of reaction (16) decomposes under light, generating in each case two radicals able to start a new radical chain:

$$ROOH + h\nu \rightarrow RO^\bullet + OH^\bullet \quad (17)$$

$$2ROOH \rightarrow RO^\bullet + H_2O + RO_2^\bullet \quad (18)$$

$$ROOH \rightarrow RO^\bullet + H_2O + R^\bullet \quad (19)$$

If $RO_2^\bullet$ is noted by p, the radical chain reaction follows the kinetics [27]:

$$p = \frac{\nu v_n}{\varphi} \times (e^{\varphi t} - 1) \quad (20)$$

where φ is the branching rate-termination; ν the radical chain length and v_n the chain radical formation rate. From Eq. (20):

$$\frac{dp}{dt} = \nu v_n e^{\varphi t} \quad (21)$$

and substituting in (16):

$$\frac{dp}{dt} = \frac{-d[R\text{-}H]}{dt} \quad (22)$$

$$\frac{d[R\text{-}H]}{dt} = -\nu v_n e^{\varphi t} \quad (23)$$

and integrating (23):

$$[R\text{-}H] = [R\text{-}H]_0 + \frac{\nu v_n}{\varphi} - \frac{\nu v_n}{\varphi} e^{\varphi t} \quad (24)$$

Substituting the experimental parameter $A = \varepsilon b[R\text{-}H]$ into Eq. (24) where k includes the terms for the molar absorption coefficient (ε) of Orange II and cell pathlength (b) then

$$A = A_0 + \frac{k}{\varphi} - \frac{k}{\varphi} e^{\varphi t} \quad (25)$$

Eq. (26) can be written down considering the term k' as k/A_0:

$$\frac{A}{A_0} = 1 + \frac{k'}{\varphi}(1 - e^{\varphi t}) \quad (26)$$

which is similar to the equation describing the radical chain reaction kinetics (Eq. (20)). Furthermore Fig. 4b shows that the term φ depends linearly on the Co^{2+}-ion concentration increasing linearly with the Co^{2+}-ion in a defined concentration range.

Fig. 5a shows the bleaching (dark) and photobleaching (under light) of an Orange II solution in the presence of Co^{2+}-ion and a significantly lower oxone concentration compared that one used in Fig. 4a. Orange II bleaching in the dark occurs within 400 s and could be fitted by zero-order decay kinetics. Ten points could be registered for the bleaching process within 200 s in the experimental set-up used for this experiment (see Fig. 1).

The photobleaching under Xe-light is seen to be considerably faster than the bleaching and was observed to be complete in ~120 s. The photobleaching trace presents a different shape than the trace found for the bleaching in the dark and can be fitted by Eq. (26) which corresponds to a branched radical chain reaction mechanism. In this case 1024 signals could be accumulated in 100 s and this is shown by the experimental photobleaching trace in Fig. 5a. The fitting of the experimental trace using Eq. (26) shows an error of less than 5% between the experimental results and the fitting procedure used. The faster photobleaching observed of Orange II suggests that light irradiation accelerates the decomposition of ROOH produced by oxone in the presence of O_2 (see Eq. (17)). This light activated decomposition of ROOH explains the faster photobleaching of Orange II with respect to the bleaching in the dark (Fig. 5a). The plot in Fig. 5b shows that the concentration of oxone has no influence on the branched radical reaction mechanism, since the branching parameter remains almost constant up to [oxone] = 40 mM.

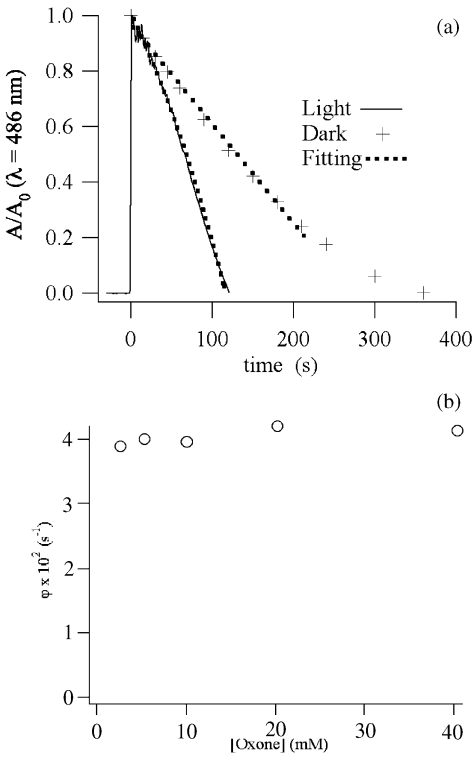

Fig. 5. (a) Bleaching and photobleaching of a solution of Orange II (0.2 mM) in the presence of oxone (2.7 mM) and Co^{2+} (0.1 mM). (b) Branching parameter plotted against the oxone concentration for the photobleaching of an Orange II (0.20 mM) solution in the presence of Co^{2+} (0.05 mM). For other details see text.

3.3. Effect of the variation of the solution parameters on the TOC decrease of Orange II solutions under visible light irradiation

Even though the bleaching of Orange II was accelerated under visible light irradiation, the TOC reduction is much slower than the bleaching/photobleaching. Fig. 6 shows that for a solution containing Orange II (0.2 mM) and oxone (20 mM), an increase in the Co^{2+}-ion concentration between 0.02 and 0.5 mM leads to an initial rate for the TOC reduction reaching the maximum of 0.42 mg Cl^{-1} min^{-1} at a Co^{2+}-ion concentration of 0.1 mM. These values for higher concentrations of Co^{2+}-ions were seen to remain constant, in Fig. 6. It is also seen in Fig. 6 that by using a concentration of 0.06 mM of Co^{2+}-ion, the maximum rate of decrease in the TOC values was attained for a solution of Orange II (0.20 mM).

Fig. 7 shows the TOC reduction for an Orange II solution in the presence of a concentration of Co^{2+}-ions (0.06 mM) under visible light as a function of oxone concentration. The initial mineralization rate (Fig. 7) was found from the slopes of the TOC reduction over the unit time (min) as a function of the added concentrations of Co^{2+}. The TOC removal rate

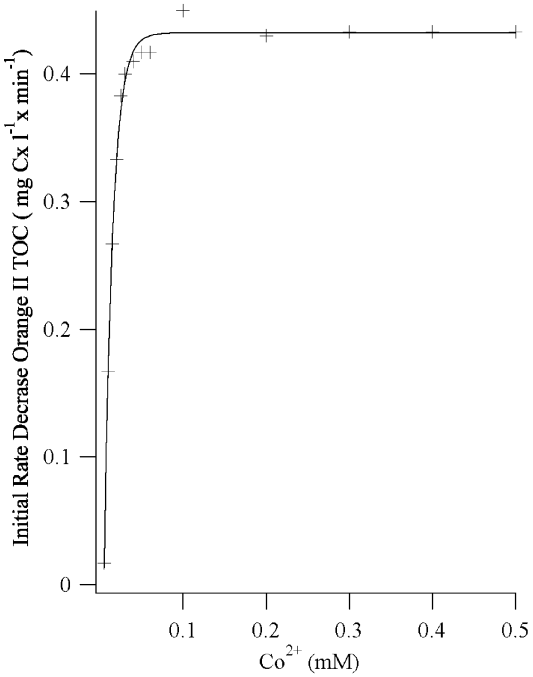

Fig. 6. Reduction of total organic carbon of an Orange II solution (0.20 mM) under Suntest simulated light (90 mW/cm^2 in the presence of oxone (20 mM)) as a function of Co^{2+}-ion concentration.

is readily seen to be independent for oxone concentrations above 5.50 mM since the mineralization rate remained the same for higher oxone concentrations indicating that at this value oxone saturation was reached for an Orange II solution (0.20 mM). The oxone necessary for the stoichiometric reaction between oxone and Orange II can be estimated to be 18.5 times the amount of dye as seen from the approximate mineralization stoichiometry of Orange II:

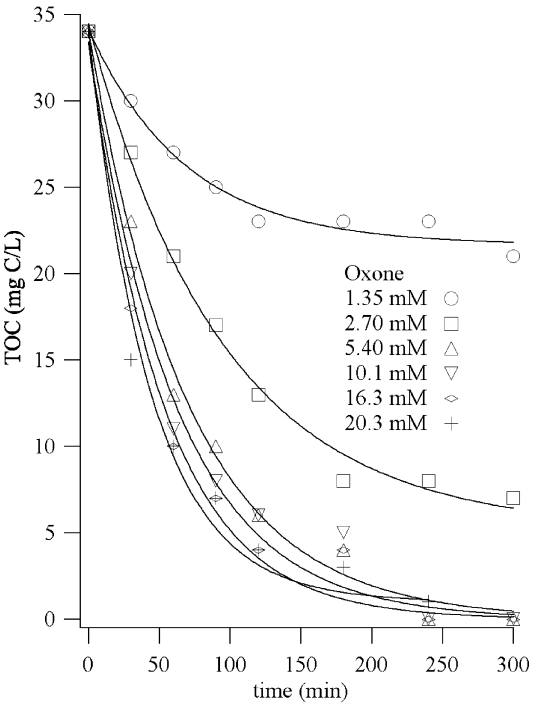

Fig. 7. Reduction in TOC for an Orange II (0.20 mM) solution under Suntest irradiation (90 mW/cm^2) in the presence of a fixed concentration of Co^{2+} (0.06 mM) as a function of oxone added in solution at pH = 2.2.

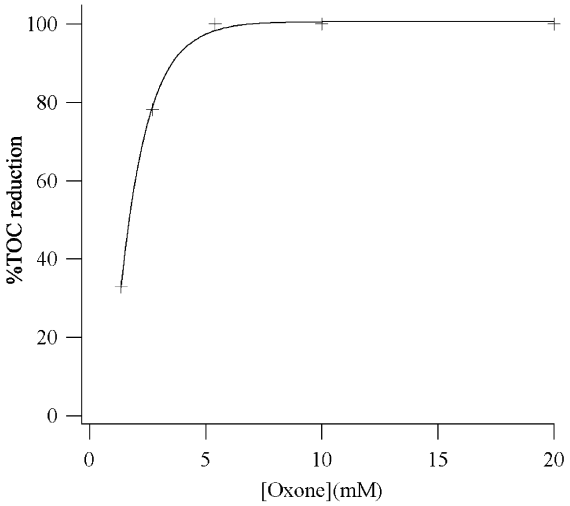

Fig. 8. Percentage of the TOC removal from an Orange II (0.20 mM) solution as a function of oxone concentration in the presence of $[Co^{2+}] = 0.06$ mM. Suntest light irradiation (90 mW/cm^2).

$$C_{16}H_{11}N_2NaO_4S + 37/2(2KHSO_5 \cdot KHSO_4 \cdot K_2SO_4) \rightarrow 16CO_2 + 5H_2O + N_2 + NaHSO_4 + 111/2KHSO_4 + 37/2K_2SO_4 \quad (27)$$

The stoichiometric amount of oxone (see Eq. (27)) is 1.66 g oxone for 2.70 millimoles of Orange II. Fig. 7 shows that an oxone concentration of 5.40 mM completely mineralizes a solution of Orange II (0.20 mM). This oxone amount is consistent with the approximate stoichiometry predicted by Eq. (27), when oxone is used as an oxidant (see Eqs. (5)–(11)). In the dark, no meaningful reduction in the TOC was found (<10%) using the experimental conditions noted in Fig. 7.

Fig. 8 shows the TOC reduction of Orange II in the presence of a sufficient concentration of Co^{2+}-ions to completely mineralize the dye (see Fig. 6), as a function of oxone concentration. Fig. 8 shows that complete mineralization of Orange II (0.20 mM) was attained using an oxone concentration of 6 mM. This latter result shows that a very low concentration of Co^{2+}-ions (0.06 mM) is necessary compared to the oxone concentration needed to catalyze the complete mineralizaion of Orange II.

Fig. 9 shows the mineralization kinetics of Orange II as the concentration of the dye is increased from 0.20 to 0.50 mM. It also shows that the initial rate of TOC removal remained the same as the concentration of Orange II in solution as increased, calculated from the first-order mineralization rate of Orange II. The inset in Fig. 9 shows the initial TOC removal rate of Orange II practically did not depend on the Orange II concentration in solution, since the variation observed in

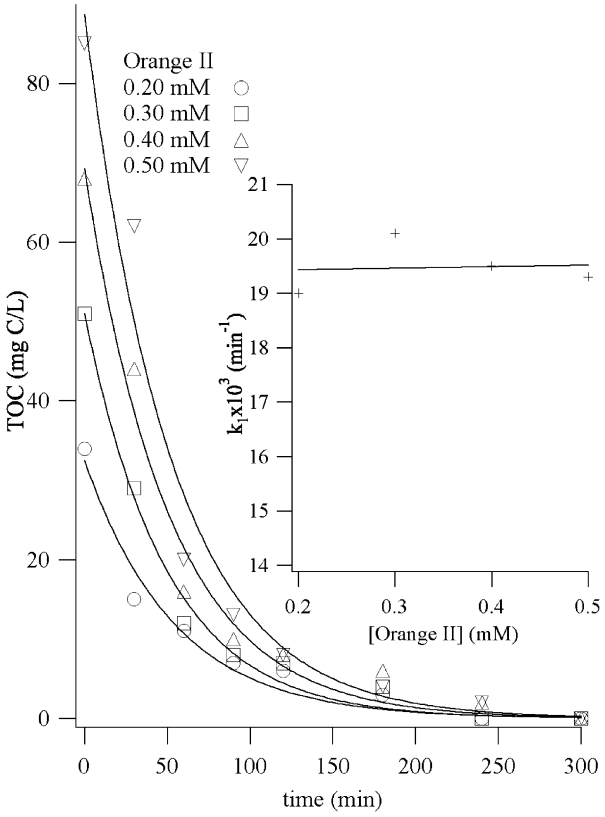

Fig. 9. Reduction in TOC for different concentrations of Orange II in the presence of Co^{2+} (0.06 mM) and oxone (20 mM) under Suntest light irradiation (90 mW/cm^2). The inset shows that of the initial TOC removal rates on the Orange II.

the TOC removal rate was within the experimental error expected in these kind of measurements. That the mineralization of Orange II proceeds for the various concentration of Orange II in ~200–300 min suggests a mass controlled type of process taking place during Orange II mineralization.

3.4. Sulfate evolution in the dark and under light when oxone + Co^{2+} catalyze Orange II mineralization

Fig. 10 shows the evolution of sulfate-ion in solutions during Orange II oxidation by oxone in the presence of Co^{2+} in the dark and under Suntest light irradiation. The evolution of the sulfate during the dark oxidation of Orange II reaches ~75% of the stoichiometric amount. But under light irradiation, 95% of the possible maximum amount of sulfate-ions was reached. Under light irradiation Orange II seems to photosensitize the oxone reaction with Co^{2+}, producing additional sulfate oxidizing radicals as reported in Fig. 10. The TOC reduction from the initially added Orange II was followed up to ~300 min and the mineralization was observed to be complete. No mineralization was observed to take place in the dark under similar experimental conditions. The sulfate content of the solution between 0 and 300 min was detected in control experiments under light irradiation when oxone was the only reagent in solution. The

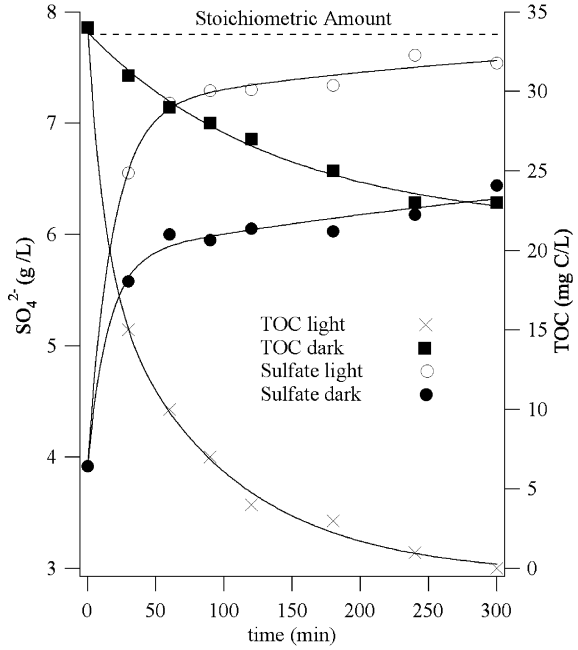

Fig. 10. Sulfate and TOC evolution in an Orange II (0.20 mM) solution in the presence of oxone (20 mM) and Co^{2+} (0.06 mM) in the dark and under Suntest light irradiation (90 mW/cm^2).

sulfate content determined in the solution in the dark, was equivalent to the sulfate content of oxone $KHSO_4{\cdot}K_2SO_4$ of 3.9 g/l and this is the initial value for the sulfate-ions noted in the left hand side in Fig. 10. But there was no stoichiometric correspondence between the SO_4^{2-} generated in the solution and the TOC reduction of Orange II in Fig. 10. This suggests a complex chain of events during Orange II oxidation by the oxone/Co^{2+} reagent as stated previously in Eqs. (5)–(9) and further discussed below in Eqs. (28)–(35).

3.5. Influence of the gas atmosphere on the Orange II mineralization under visible light irradiation

Fig. 11 presents the TOC reduction for Orange II solutions saturated with different gases. It is readily seen that mineralization is favored in oxygen saturated solutions and is complete after ~90 min. Fig. 10 shows that it takes ~90 min to evolve the maximum amount of sulfate-ions under light irradiation. Orange II is seen not to be completely mineralized in Ar purged solutions and at a much longer time in air purged solutions. It can be concluded that during the first 30 min the oxone acts as the dominant oxidant in solution and only in a second reaction step does the formation of peroxides contributes in an important way to the mineralization of Orange II. The contribution of peroxides to the Orange II degradation suggested in Section 3.2 is outlined below incorporating the evidence found in Sections 3.3–3.6:

$$\text{Orange II} + h\nu \rightarrow \text{Orange II}^* \quad (28)$$

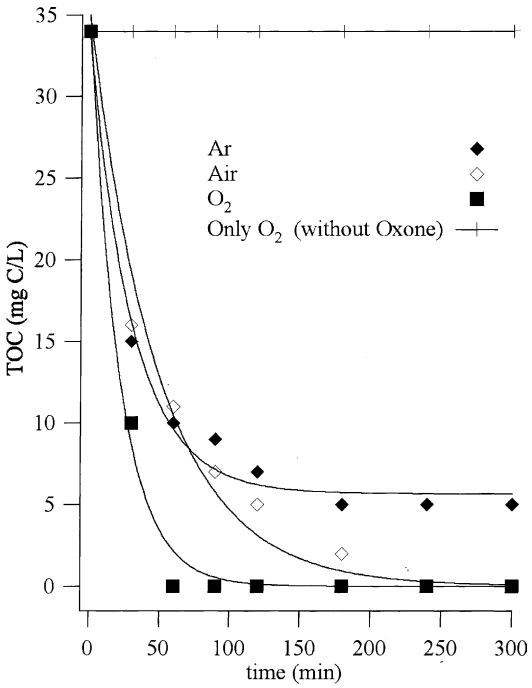

Fig. 11. Reduction in TOC for Orange II solutions (0.20 mM) in the absence and in the presence of oxone (20 mM) and Co^{2+} (0.06 mM) under Suntest light irradiation (90 mW/cm^2). Different gases are used to saturate the solution during the light irradiation.

$$\text{Orange II}^{*} + \text{oxone} \rightarrow \text{Orange II}^{\bullet} + (\text{HO}^{\bullet} + \text{SO}_4{}^{2-} \quad \text{or} \quad \text{HO}^{-} + \text{SO}_4{}^{\bullet -}) \tag{29}$$

$$\text{degraded product} + \text{Co}^{3+}/\text{HO}/\text{SO}_4{}^{\bullet -} \rightarrow \text{radical intermediate (R}^{\bullet}) \tag{30}$$

$$\text{R}^{\bullet} + \text{oxone}/\text{O}_2 \rightarrow \text{CO}_2 + \text{H}_2\text{O} \quad (\text{R}^{\bullet} \text{ is the radical Orange II}) \tag{31}$$

$$\text{R}^{\bullet} + \text{O}_2 \rightarrow \text{R-OO}^{\bullet} \tag{32}$$

$$\text{ROO}^{\bullet} + \text{RH} \rightarrow \text{ROOH} + \text{R}^{\bullet} \tag{33}$$

$$\text{ROO}^{\bullet} + \text{ROO}^{\bullet} \rightarrow \text{ROOR} + \text{O}_2 \tag{34}$$

$$\text{R-OOH} + h\nu \rightarrow \text{RO}^{\bullet} + \text{OH}^{\bullet} \tag{35}$$

The dissolved oxygen seems to play an active role leading to peroxy-radicals, ROO$^{\bullet}$ (R = H, alkyl, aryl) [24–26] and peroxy-radicals serve as chain propagators and oxidize organic materials either by hydrogen abstraction or electron transfer process [28–30]. Under light irradiation, the additional generation OH$^{\bullet}$-radicals improve the kinetics of the Orange II mineralization (20) as reported earlier for Fenton systems [7,26]. A TOC reduction from 34 to 15 mg C/l (Fig. 11) was observed within 30 min and this corresponds to a stoichiometric increase of 2.63 g/l sulfate in Fig. 10. But an increase of 0.35 g/l in the sulfate-ion concentration has only been observed. A considerable fraction of the $HSO_5{}^{-}$ (see Eq. (27)) is seen to be lost by reaction channels that are not directly related to the mineralization of Orange II.

4. Conclusions

Accelerated bleaching and mineralization of Orange II taken as a model system is reported using the novel Co^{2+}/oxone reagent in the dark and under light. The photobleaching of Orange II under Xe-light was faster than the bleaching (dark). The light induced decomposition of the ROOH produced during the degradation of Orange II by the Co^{2+}/oxone reagent seems to be responsible for the faster photobleaching of the dye compared to the bleaching observed in the dark. The photobleaching profile presented a different shape compared to the bleaching trace and can be fitted by a single mathematical expression which corresponds to a branched radical chain reaction mechanism. The dependence of the photobleaching and mineralization of Orange II on the oxone and the Co^{2+}-ion concentration was investigated. The beneficial effect of O_2 during the mineralization of Orange II due to the formation of peroxide radicals was noticed when solutions containing Co^{2+}/oxone were purged with O_2 as is the case in Fenton-like reactions. A mechanism for this observation is suggested, consistent with the experimental observations.

Acknowledgements

The financial support for this study by the KTI/CTI TOP NANO 21 (Bern, Switzerland) under grant No. 6116.4 TNS is duly appreciated.

References

[1] A. Reife, H. Freeman, Environmental Chemistry of Dyes and Pigments, Wiley/Interscience, New York, 1996.
[2] M. Hoffmann, M. Martin, W. Choi, D. Bahnemann, Chem. Rev. 95 (1995) 69.
[3] J. Fernandez, J. Bandara, A. Lopez, Ph. Buffat, J. Kiwi, Langmuir 15 (1999) 185.
[4] M.R. Dhananjeyan, E. Fine, J. Kiwi, J. Photochem. Photobiol. A: Chemistry 136 (2000) 125.
[5] V. Sarria, S. Parra, N. Adler, P. Peringer, N. Benitez, C. Pulgarin, Catal. Today 76 (2002) 301.
[6] C. Morrison, J. Bandara, J. Kiwi, J. Adv. Oxid. Technol. 1 (1996) 160.
[7] J. Kiwi, A. Lopez, V. Nadtochenko, Environ. Sci. Technol. 33 (1999) 1832.
[8] D.F. Ollis, H. Al-Ekabi, Photocatalytic Purification and Treatment of Water and Air, Elsevier, Amsterdam, 1993.
[9] M. Halmann, Photodegradation of Water Pollutants, CRC Press, Boca Raton, FL, 1996.
[10] M.R. Dhananjeyan, E. Fine, J. Kiwi, J. Photochem. Photobiol. A 136 (2000) 125.
[11] S. Malato, J. Blanco, C. Richter, B. Braun, M.I. Maldonado, Appl. Catal. B: Environ. 17 (1998) 347.

[12] R. Renganathan, P. Maruthamuthu, Int. J. Chem. Kinet. 18 (1986) 49.
[13] F. Campaci, S. Campestrini, J. Mol. Catal. A: Chem. 140 (1999) 121.
[14] J. Legros, B. Crousse, J. Bourdon, D. Bonnet-Delpon, J.-P. Begue, Tetrahedron Lett. 42 (2001) 4463.
[15] S. Tsukada, H. Miki, J.-M. Lin, T. Suzuki, M. Yamada, Anal. Chim. Acta 371 (1998) 163.
[16] P. Neta, R. Huie, A. Ross, J. Phys. Chem. Ref. Data 17 (1988) 513–886.
[17] G. Manivannan, P. Maruthamuthu, Eur. Polym. J. 23 (1987) 311.
[18] P. Maruthamuthu, M. Ashok Kumar, L. Venkatasubramanian, Bull. Chem. Soc. Jpn. 61 (1988) 4137.
[19] P. Maruthamuthu, K. Gurunathan, E. Subramanian, M. Ashok Kumar, Bull. Chem. Soc. Jpn. 64 (1991) 1933.
[20] J. Beltran, R. Ferrus, Ann. Roy. Soc. Esp. Fis. Quim., Ser. B 61 (1965) 515.
[21] J. Kim, J.O. Edwards, Inorg. Chim. Acta 235 (1995) 9.
[22] R. Connick, Y. Zhang, S. Lee, R. Adamic, P. Chieng, Inorg. Chem. 34 (1995) 4543.
[23] K. Laidler, Chemical Kinetics, McGraw-Hill, Toronto, 1985, and references therein.
[24] R.C. Thompson, Inorg. Chem. 20 (1981) 1005.
[25] V. Nadtochenko, J. Kiwi, J. Chem. Soc., Faraday Trans. 93 (1997) 2373.
[26] B. Ruppert, R. Bauer, G. Heisler, J. Photochem. Photobiol. A 73 (1993) 75.
[27] N. Emanuel, D. Kmorre, Cinetique Chimiques, Mir, Moscow, 1975.
[28] A. Meenakshi, M. Santappa, J. Catal. 19 (1970) 300, and the references therein.
[29] B. Maillard, K.U. Ingold, J.C. Scaiano, J. Am. Chem. Soc. 105 (1983) 5095.
[30] K.U. Ingold, Acc. Chem. Res. 2 (1969) 1.